Master's Thesis

석사 학위논문

Gβγ-dependent modulation of ion channels

Christina Dasom Baek (백 다 솜 白 다 솜)

Department of Brain Science

뇌과학전공

DGIST

2013

Master's Thesis

석사 학위논문

Gβγ-dependent modulation of ion channels

Christina Dasom Baek (백 다 솜 白 다 솜)

Department of Brain Science

뇌과학전공

DGIST

2013

Gβγ-dependent modulation of ion channels

Advisor : Professor Byung-Chang Suh

Co-advisor : Sang-Jun Moon

by

Christina Dasom Baek

Department of Brain Science

DGIST

A thesis submitted to the faculty of DGIST in partial fulfillment of the requirements for the degree of Master of Science in the Department of Brain Science. The study was conducted in accordance with Code of Research Ethics[1].

11/15/2013

Approved by

Professor Byung-Chang Suh   _____
(Advisor)

Professor Sang-Jun Moon   _____
(Co-advisor)

---

[1] Declaration of Ethical Conduct in Research; I, as a graduate student of DGIST, hereby declare that I have not committed any acts that damage the credibility of my research. These include, but are not limited to: falsification, thesis written by someone else, distortion or research findings or plagiarism. I affirm that my thesis contains honest conclusions based on my own careful research under the guidelines of my thesis advisor.

Gβγ-dependent modulation of ion channels

Christina Dasom Baek

Accepted in partial fulfillment of the requirements for the degree
of Master of Science

11.15.2013

Head of Committee   _____   (Signature)

Prof. Byung-Chang Suh

Member of Committee _____   (Signature)

Prof. Sang-Jun Moon

Member of Committee _____   (Signature)

Prof. Eun-Kyoung Kim

Abstract

Ion channels selectively allow ions to pass in or out of cells and are exquisitely sensitive to modulation by specific G protein-coupled receptors. This gives excitable cells the ability to undergo and regulate dynamic alterations in membrane potential to perform critical biological functions. Specialized voltage-gated calcium channels, $Ca_V2.2$ (N-type) channels and G protein-coupled potassium 2A channels (GIRK2A) are both regulated by the direct binding of Gβγ protein dissociated from the $G_{i/o}$-protein-coupled receptors ($G_{i/o}$PCRs). The focus of this study lies within this fast, voltage-dependent, and membrane delimited mechanism of ion channel modulation. In the first section, the possible existence of this pathway following the activation of a G_qPCR is explored. Previous studies have demonstrate the distinct pathway of inhibition following G_qPCR activation to be mostly due to a slow, voltage-independent, lipid-dependent pathway. However the exclusivity of this traditionally believed mechanism is questioned with the possibility of Gβγ involvement. The results clearly defend this hypothesis. A significant reduction in $Ca_Vβ2a$ current inhibition was recorded with cells pre-incubated with PTX and expressing. PTX is a $G_{i/o}$PCR and thus Gβγ blocker which suggests Gβγ also has a role in the G_qPCR mediated inhibition of $Ca_V2.2$ channels. In the second section, the significance of two electrostatic residues recently found to be present within the binding interface of GIRK2A subunits and Gβγ, but not GIRK1 subunits is explored. Using molecular biology techniques, site-directed mutagenesis has been performed to produce two mutations of the GIRK2 channel, E350K (negative to positive) and E358A (negative to hydrophobic). Both these mutations resemble the amino acids present in GIRK1 which have been shown to contribute to the binding interface between the two proteins. This is particularly interesting as GIRK channels are the only channels known to be activated upon Gβγ binding among the large group of potassium ion channels. The reason for this difference is still not well understood. The results illustrate a significant decrease in this GIRK2A mutant current activation which indicates the significance of the conserved residues. Furthermore, GIRK1 is a crucial subunit in physiology, as GIRK channels exist more abundantly as heterotetramers of GIRK1/2 in the brain and GIRK1/4 in the heart. Exploring the detailed mechanism of its activation through the binding of Gβγ is therefore a relevant subject of interest. The results present a distinct decrease in activation extent of the GIRK2 channel mutants relative to that of the wild-type however, change in the activation kinetics was not observed.

Keywords : Calcium ion, potassium ion, Gβγ protein, regulation, electrophysiology

Table of Contents

Chapter 1: Gβγ has a significant part in G_qPCR mediated inhibition of $Ca_V2.2$ channels

Chapter 2: Electrostatic residues in the Gβγ-dependent inhibition of GIRK2A channels

List of Figures

Chapter 1: Gβγ has a significant part in G_q-PCR mediated inhibition of $Ca_V2.2$ channels

Chapter 2: Electrostatic residues in the Gβγ-dependent inhibition of GIRK2A channels

Chapter 1: Gβγ has a significant part in G_qPCR mediated inhibition of $Ca_V2.2$ channels

1. INTRODUCTION

Ion channels are essential in maintaining and dynamically altering the membrane potential of all excitable cells. They act as a pathway for ions such as calcium, sodium and potassium to pass through the lipid barrier of the cell membrane. This process is especially critical in the study of neuroscience as the communication from one neuron to multiple other neurons and thus the entire neural network is based on this electrical transmission of action potential and thus subsequent release of neurotransmitters at the interface of two neurons, called the synapse [1].

Ion channels can be activated upon many types of stimuli such as chemical ligands, change in the membrane potential, pH and even mechanical influences. Furthermore, these ion channels are modulated by an array of regulating factors. These include specific G-protein-coupled receptors (GPCRs) [2], lipid molecules in the membrane [3, 4], signaling ions themselves, downstream intracellular effectors and much more [5]. The importance of controlling the activity of ion channels can be deduced from the vigorous changes that occur following the opening or closing of such channels. In the brain, this in turn can lead to vast changes in synaptic plasticity as the release of neurotransmitter following changes in intracellular ionic levels can be directly affected [6].

The ion channels section of the paper are voltage-gated calcium (Ca$_V$) channels. These channels play a crucial role in many types of excitable cells by allowing the specific influx of calcium of into the cell [7]. This subsequently results in the depolarization following Ca$_V$ channel activation [8]. This has several physiological implications. It is well known that the dysfunction in ion channels is associated with many diseases, both in the development and the progression stages. Some examples include, epilepsy due to the decrease in Ca$_V$ activity, ataxia, paralysis, obesity and even cancer progression [9] [10].

All calcium channels consist of many subunits, including the α1, α$_2$δ-1 and β subunits [11]. The α subunit contains the major structural features needed for permeation, activation and inactivation of the channel. In the mammalian genome, ten different types of a subunits are encoded and this is what categorizes the channels into three major families; Ca$_V$1 (L-type channels), Ca$_V$2 (N, P/Q and R-types) and Ca$_V$3 (T-type) [12]. The channel of focus in this study, is the Ca$_V$2.2 which is part of the high-voltage activated calcium channels. This channel along with Ca$_V$2.1 is prominently drives neurotransmitter release in the synapse. This thus highlights the many implications associated with these channels following their dysfunctions in not only neurological diseases but also in other systems where excitable cells are present, such as in the musculatory system [13].

Many ion channel, including the calcium channel of interest are regulated by the activation of G-protein coupled receptors (GPCRs). GPCRs are seven-transmembrane receptors which are abundantly distributed type of receptor, which is involved in the regulation of both of these channels [14] [15] [16]. GPCRs are activated by the binding of a specific ligand to the extracellular portion of the receptor [14]. This causes the coupling of the intracellular G protein to bind which undergoes hydrolysis to dissociate to Gα and Gβγ proteins. These two proteins act as second messengers within the cell to initiate a signaling cascade. There are many types of GPCRs with stimulatory and inhibitory downstream effects [17]. Two GPCRs explored in this study are the G$_{i/o}$PCRs and G$_q$PCRs [18].

Many previous studies have demonstrated the distinct regulatory mechanism by which Ca$_V$2.2 are inhibited differentially according to the type of GPCR activated. These pathways can be divided into two

large groups. The fast voltage-dependent pathway is mediated by $G_{i/o}$-coupled protein receptors ($G_{i/o}$PCR), due to the direct binding of liberated $G\beta\gamma$ protein to the recipient calcium ion channel and thus decrease in calcium influx [19] [20]. In contrast, the binding of a ligand to the G_qPCR has been described in many papers to involve the depletion of PIP_2 from the membrane following $G\alpha$ subunit dissociation from G-proteins and activation of phospholipase C (PLC). This results in the production of inositol 1,4,5-triphosphate (IP_3) and diacyglycerol (DAG) from PIP_2 and thus activation of downstream signaling cascades to inhibit $Ca_V2.2$ [21] [22, 23] [24].

In a recent paper on the modulation of high-voltage gated channels, it was apparent that the total inhibition resulting from G_qPCR activation, was not equivalent to that of the inhibition resulting from depletion of PIP_2 through the use of Dr-VSP [25] [26]. This suggested that another mechanism may be functioning to inhibit these channels, other than the well-established PIP_2-dependent pathway. This study explores the hypothesis of a possible $G\beta\gamma$ role in the inhibition of calcium 2.2 channels by G_qPCRs by using electrophysiological techniques to record the effects of PTX, a pertussis toxin which inhibits the $G_{i/o}$PCRs and therefore inhibited the $G\beta\gamma$ subunit function in activated G_qPCRs.

2. MATERIALS AND METHODS

2.1. Expression of calcium channels in mammalian cell lines

To study the $Ca_V2.2$ channel, the relevant genes were transfected into mammalian cell lines for expression.

2.1.1. Mammalian cell lines

For studying the $Ca_V2.2$ channels, cDNAs encoding channel subunits, rat α1B, α2δ1 and β3 (37b), (a gift of

Diane Lipscombe, Brown University, Providence, RI), β2a (from William A. Catterall, University of

Washington, Seattle, WA), M1-muscarinic (from Neil N. Nathanson, Univeristy of Washington, WA),

human M2-Muscarinic receptor (from Guthrie Resouce Centrer, Rolla, MO) and voltage-sensing lipid

phosphatase from zebrafish (Dr-VSP) with internal ribosome entry site EGFP (from Yasushi Okamura,

Osaka University, Osaka, Japan) all harbored in mammalian expression vectors were heterogously-

expressed by transfecting into human embryonic kidney cell line derivative tsA201-cells (HEK tsA-201

cells). tsA201 cells do not contain detectable levels of endogenous calcium channel subunits and thus

serves as an appropriate surrogate for examining the *in vitro* expressed channels. These cells are a highly

transfectable derivative of the 293 cell line into which a stably plasmid containing the SV40 large T

antigen is integrated. This maintain a high copy number of plasmids expressed episomally, such as

vectors used in this study (pcDNA) which contain the SV40 mammalian origin of replication.

2.1.2. Passage of tsA201 cell Line

tsA201 cells were grown on standard complete medium (DMEM supplemented with 10% Fetal Bovine

Serum (FBS) and 0.2% penicillin/streptomycin as a monolayer in disposable sterile 100 mm petri dishes

(diameter) to 80% confluency at 37°C in a CO_2 (5%) incubator. Every 3-4 days, tsA201 cells were

passaged to a new dish by 1:10 dilution. To detach the cell line, cells were treated with 1 mL of trypsin,

incubated at 37°C for 30 s before adding 10 mL of complete media to inactivate the trypsin. Resuspended

culture not used for maintaining the new passage were replated to 30 mm (diameter) sterile petri dishes for ready for transfection. DMEM, FBS, and penicillin/streptomycin were obtained from Invitrogen.

2.1.3. Lipofectamine transfection

Lipofectamine™ 2000 Transfection Reagent from Invitrogen, is a proprietary cationic lipid formulation which offers high transfection efficiency and protein expression levels for tsA201 cells [27]. The tsA201 cells were allowed to settle on 30 mm petri-dishes to 70% confluency for at least a 24 hours. 20 μL of lipofectamine reagent in 250 μL of pure DMEM was mixed with relevant amounts of DNA (Less than 10 μg) which was also added to 250 μL of pre DMEM. Both solutions were mixed and incubated in room temperature for 15 minutes before adding the transfectant mixture to cell culture dishes with an additional 1500 μL of DMEM. These cells were transferred to coated Poly-L-Lysine coated chips the next day and studied within 1 – 2 days in electrophysiological experiments.

For calcium channel expression, 0.4 μg of α1B, 0.4 μg of α2δ1, 0.35 μg of β2a or β3 subunits were transfected. The relevant receptors 0.8 μg of M1R or M2R, 0.8 μg Dr-VSP and 0.1 μg of dsRed a fluorescent marker were also transfected as required.

2.1.4. Transfer of transfected tsA201 cells to Poly-L-Lysine coated chips

Transfected tsA201 cells were detached using 200 μL of trypsin and incubated at 37°C for 30 s before adding 2 mL of complete media to inactivate the trypsin. Resuspended cells were added to new sterile 30 mm petri dishes containing 8 Poly-L-Lysine coated chips.

2.2. Electrophysiological Recordings

Electrophysiological method recordings, using the whole cell patch clamping mode was conducted to study the activity of ion channels in cell membranes. The basic theoretical principle is explained in section 2.2.2.

2.2.1. Solutions and Materials

To measure the calcium channel current by the whole cell patch clamping technique, transfected tsA201 cells were bathed and recorded in external Ringer's solution containing barium as the charge carrier. Barium is used as it passes through the calcium ion channels more easily and so produced twice as large sized currents than calcium. Furthermore, barium does not interfere with the calcium-dependent intracellular cascades. The external calcium ringers solution contained 150 mM NaCl, 10 mM $BaCl_2$, 1 mM $MgCl_2$, 10 mM Hepes, and 8 mM glucose, adjusted to a pH of 7.4 with NaOH. The ground electrode was coated in $AgCl_2$.

The pipette solution contained 175 mM CsCL, 6 mM $MgCl_2$, 5 mM Hepes, 0.1 1,2-bis(2-aminophenoxy)ethane N.N.N',N'-tetraacetic acid (BAPTA), 3 mM Na_2-ATP and 0.1 mM Na_3GTP, titrated to a pH of 7.4 with CsOH. BAPTA, was obtained from Invitrogen, Oxotremorine-M (Oxo-M) was obtained from Research Biochemicals and other chemicals from Sigma.

2.2.2. Whole cell recording

The patch-clamp technique is a method developed by inventors, Bert Sakmann and Erwin Neher in 1981 which lead to the opening of a new field in electrophysiology and their Nobel Prize Award in 1991 [28]. The basic idea lies within the fact that a seal is formed with the glass microelectrode and surface of the cell [29].

The whole cell patch clamp mode was used to record and analyze the current passing through the calcium ion channels in the cell membrane. The two major advantages of this mode is that it present much less noise in recordings due to the high resistance of the glass-membrane seal and also much better voltage-clamping of the interior of the cell due to the relatively large tip diameter of the patch electrode. This thereby allows much more accurate recording of fast currents owing to the stability of the voltage-clamp. Diagram 1 illustrates this whole cell patch clamp mode where the pipette is one with the entire cell [30].
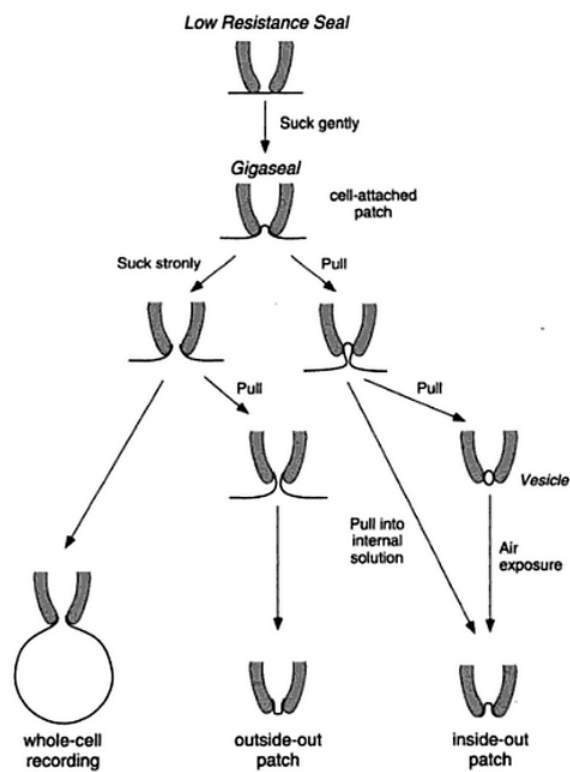
.

Diagram1. Patch-clamp recording configurations

Cells successfully transfected with calcium channels were identified by red fluorescence, emitted by RFP due to the transfected dsRed gene.

Patch pipettes (1.3 – 2.5 MOhms) were pulled from glass micropipette capillaries and filled with the pipette solution to carry out a recording. A patch of the cell membrane was sealed and ruptured by this pipette. The whole-cell access resistance was 2 – 5 MΩ, and series-resistance errors were compensated > 60%. Fast and slow capacitances were compensated before the applied test-pulse sequences. Recordings were performed using a HEKA EPC-9 amplifier with Pulse software (HEKA Elektronik).

To study the activity of calcium channels, barium currents were recorded by holding the cell at -80 mV and applying 10-ms test pulses to +10 mV. In all experiments where barium currents were measured with a 10-ms test pulse, the full protocol induced p/5 subtraction of leak and capacitive currents.

2.2.3. Data analysis

Data acquisition and analysis used Pulse/Pulse Fit 8.11 software in combination with an EPC-9 patch clamp amplifier (HEKA). Further data processing was performed with Excel (Microsoft) and Igor Pro (Wavemetrics, Inc.). Time constants were measured by exponential fits. All quantitative data are expressed as the mean ± SEM.

3. RESULTS AND DISCUSSION

3.1. $G_{i/o}$ and G_qPCR inhibition of Ca$_V$2.2(β2a) channels

To characterize the size of Ca$_V$2.2(β2a) inhibition following G_qPCRs and $G_{i/o}$PCRs, tsA201 cells were transfected with Ca$_V$ subunits α1B, β2a and α2δ1 and either M1- or M2-muscarinic receptors. Inhibition of current was evoked by the activation of either GPCRs with the perfusion of a specific agonist, Oxotremorine-M (Oxo-M). A time-course recording of Ca$_V$2.2(β2a) current illustrated a fast decrease in calcium current reflecting rapid closing of the channels following receptor activation (Figure 1, *A* and *B*). The inhibited channels remain closed until the Oxo-M perfusion ceases then recovery of current is apparent. As a control, cells transfected with no muscarinic receptors were also compared (Figure 1 *C*). No inhibition of current was observed although a significant size of calcium current was present. Figure 1 *B* represents single current traces before (a) and after (b) the addition of Oxo-M. The traces show the characteristic shape of Ca$_V$2.2(β2a) currents and it is clear from the overlaid traces (a and b) that the size of the current dramatically reduced in size following GPCR activation.

The voltage-dependent property and IV relation was compared for Ca$_V$2.2(β2a) currents in all three conditions (Figure 1 *C*). The IV curve displays the relative current sizes at increasing voltages from -50 mV in 10 mV steps. The general shape of the curve, is similar between the three plots and the peak calcium current can be observed at +10 mV for all conditions, which is typical for Ca$_V$2.2 channels.

The G_qPCR mediated inhibition of Ca$_V$2.2(β2a) exhibited a smaller percentage inhibition at 43 ± 5% (n=7) than that of $G_{i/o}$PCR mediated inhibition, which was averaged to be 55 ± 7% (n=6). As expected, for the control experiment with no muscarinic receptor expression, close to no current inhibition was observed (1 ± 0.6%, n=3). Figure 1 *D* presents the quantitative data for the percentage inhibition by Oxo-M following the absence or activation of various muscarinic receptors.

This demonstrates the prominent function of GPCRs in inhibiting the $Ca_V2.2(\beta2a)$ current. The difference in extent of percentage current inhibition following the two types of GPCRs may be due to the difference in modulatory pathways by which these receptors act. $G_{i/o}$PCRs have been established to strongly inhibit $Ca_V2.2$ channels via the binding of $G\beta\gamma$ protein to the channel itself, inhibiting the current directly. In contrast, G_qPCRs are thought be acting through the lipid dependent pathway where the $G\alpha_q$-protein initiates a signaling cascade to deplete membrane PIP_2 and lead to the indirect inhibition of $Ca_V2.2$ channels.

3.2. The lipid-dependent component of GPCR mediated inhibition

The lipid-dependent pathway of inhibition is believed to account for the majority of $Ca_V2.2$ inhibition following the activation of the G_qPCRs. This mechanism can be explored using the voltage-sensitive phosphatase from zebra fish (Dr-VSP) which quickly and reversibly depletes PIP_2 from the membrane upon a large depolarizing pulse (Pulse protocol in Figure 2 *A*). Ca^{2+} current is recorded before and after this a 120 mV pulse for 1 s to activate the Dr-VSP, to compare the current size before and after PIP_2 depletion. The hyperpolarization pulse was added after the depolarization pulse to compare if the voltage-dependent inhibition was interfering with the $Ca_V2.2$ channel inhibition. Figure 2 *C* shows little or minimal difference between the percentage of current inhibition following activation of Dr-VSP, in the absence and presence of a hyperpolarization pulse. This suggests the external factor of voltage-dependent inhibition of $Ca_V2.2(\beta2a)$ and $Ca_V2.2(\beta3)$ was not present.

The percentage of $Ca_V2.2(\beta2a)$ inhibition following Dr-VSP activation (taken from the protocol with no hyperpolarization) was measured to be $18 \pm 5\%$ (n=4) (Figure 2 *D*). Compared to the percentage inhibition of $Ca_V2.2(\beta2a)$ following activation of M2R, the voltage-dependent $G_{i/o}$PCR, the depletion of PIP_2 only made up for a small portion of the total current inhibition. However, the size of this lipid-dependent inhibition compared to the size of total inhibition following G_qPCR activation, only made up for around half of the total inhibition percentage (Compared to $43 \pm 5\%$ following M1R activation). This

suggested the presence of another regulatory mechanism by which G_qPCRs function to inhibit $Ca_V2.2(\beta2a)$, other than the lipid-dependent pathway.

This comparison was also applied to cells expressing $Ca_V2.2(\beta3)$ channels. The G_qPCR and $G_{i/o}$PCR mediated modulation of $Ca_V2.2(\beta3)$ was also recorded (Figure 2 *B*). Similar patterns of current inhibition upon addition of Oxo-M was observed. Quantitative comparison show that the inhibition of $Ca_V(\beta3)$ is much more robust at 77 ± 6% (n=3) inhibition following M2R activation and 57 ± 12% inhibition following M1R activation (Figure 2 *E*).

From these results it seems that the $Ca_V(\beta3)$ channels are more sensitive to the lipid-dependent pathway when inhibited by the M1Rs and the Dr-VSP induced inhibition of these channels seem to make up for most of the inhibition by M1R. As a control, M2R activation causes voltage-dependent inhibition and so the is much larger than that of the inhibition induced by the lipid-dependent pathway.

3.3. PTX effects on the $G_{i/o}$PCR induced inhibition of $Ca_V2.2(\beta2a)$

The role of pertussis toxin (PTX), a potent inhibitor of $G_{i/o}$ proteins was examined in relation to the modulation of $Ca_V2.2(\beta2a)$ channels. PTX functions by stunting the $G\beta\gamma$-dependent inhibition of $Ca_V2.2$ by specifically catalyzing the ADP-ribosylation of the $G_{i/o}$ protein and thus preventing its interaction with the receptor [31]. To confirm its function and quantify the extent of this effect, cells were co-transfected with $Ca_V(\beta2a)$ and M2-muscarinic receptor, a $G_{i/o}$PCR which predominantly functions through the $G\beta\gamma$ protein. These cells were pre-incubated with PTX for 12-16 hours prior to electrophysiological recordings. The results confirmed the PTX effect on current inhibition as with this toxin, the percentage of inhibition following M2R activation was reduced from ~55% to 4 ± 1% inhibition (n=7) (Figure 3 *A, D*).

To check for possible adverse effects of PTX, the denatured form of PTX (iPTX) was tested in the same condition (Figure 3 *B*). Pre-incubation with iPTX only resulted in a slightly reduced level of current inhibition to 41 ± 3%. Furthermore, PTX incubated with only $Ca_V2.2(\beta2a)$ channels and no receptor

showed very little current inhibition, 4 ± 1% (Figure 3 *C*). These results confirm the effect of PTX on the $G_{i/o}$- protein and it can be deduced that the Gβγ, unable to dissociate from the G-protein was unable to function to induce current inhibition.

3.4.   PTX effects on the G_qPCR induced inhibition of $Ca_V2.2(β2a)$

Using the PTX function established in the previous section, an attempt was made to identify a possible alternative mechanism by which inhibition of $Ca_V2.2$ occurs following G_qPCR activation. Cells were co-transfected with $Ca_V2.2(β2a)$ and M1R and pre-incubated with PTX using the same procedure. A substantial decrease in percentage inhibition was observed (Figure 4 *A*). The comparison with the control quantifies this difference (Figure 4 *D*). M1R alone showed ~40% inhibition of calcium current, however, with PTX, this was reduced to 21 ± 2%. This provides strong evidence that the inhibition of $Ca_V2.2(β2a)$ is at least in part mediated by the effect of the Gβγ protein dissociated from the G_qPCR.

To ensure that this effect was not due to any other external factors, the inhibition of $Ca_V2.2(β2a)$ in the presence of denatured PTX (iPTX) was also tested. iPTX was treated to cells co-expressed with the same DNA of $Ca_V2.2(β2a)$ and M_1R, 12 – 16 hours before current was recorded (Figure 4 *B*). Calcium current was inhibited by 32 ± 2 % in this condition (Figure 4 *D*). This proved not to be as large as the inhibition of current in control situations; the difference when the error bars were considered was not significant. Furthermore, PTX in the absence of a muscarinic receptor resulted in very little inhibition of current, which suggested PTX did not have considerable adverse effects (Figure 4 *C*).

Thus, this provides some evidence that, not only the conventionally understood lipid-dependent pathway of G_qPCR is present, in inhibiting $Ca_V(β2a)$ but also the voltage-dependent, Gβγ mediated inhibition as well. This is challenges the differentiation of signaling pathways following activation of distinct GPCRs. This provides further, multiple questions to be posed. If this specificity is not as distinct between the type of GPCR activated and the signaling pathway which follow, the role of each G protein can be questioned in all GPCR signaling pathways modulating not only calcium channels but various other associated channels.

A deeper understanding of the GPCR signaling pathways regulating channels, in this case calcium channels is critical in understanding the physiology and related diseases or conditions. This is because the regulation of these robustly acting channels is a method by which these channels can be manipulated and/or fixed to address such conditions for ultimately therapeutic intervention.

4. FIGURES LEGENDS

Figure 1. GPCR Modulation of Ca$_V$(β2a) channels

(A) tsA201 cells transfected with Ca$_V$ α1B (Ca$_V$2.2), α2δ1, β2a and M1R (Left) or M1R (Right) or no muscarinic receptor were recorded. Whole-cell Barium current recordings during 10 μM Oxo-M perfusion onto cells. (B) Current traces of recordings before and after Oxo-M application. (C) IV curve of Ca$_V$2.2 in cells co-expresing M1R (red), M2R (Blue) and in the absence of a receptor (Black). (D) Summary of muscarinic suppression of Ca$_V$2.2 currents with β2a.

Figure 2. Regulation of Ca$_V$2.2 channels by PIP$_2$ depletion

(A) Cells transfected with Ca$_V$ β-subunit β2a and β3 co-transfected with α1B, α2δ1 and Dr-VSP received a test pulse (a), then a depolarization to +120 mV for 1 s, hyperpolarization to -150 mV for 0.4 s, and a second test pulse (b) as shown in the protocol (Upper). The current before (a) and after (b) the depolarizing pulse are presented (Lower). (B) Sumamry of Ca$_V$2.2 current inhibition (%) by the strong depolarizing pulse in cells expressing Dr-VSP with Ca$_V$2.2 and β3- or β2a-subunits.

Figure 3. PTX effects on M2R mediated inhibition of Ca$_V$2.2(β2a).

(A) Time series recording of cells expressing M1R and Ca$_V$(β2a) was recorded after pre-incubation in PTX. M2R activation by Oxo-M (10 μM). (B) Ca$_V$(β2a) inhibition by M1R following pre-incubation in iPTX. (C) Ca$_V$(β2a) inhibition by M1R following PTX incubation in the absence of PTX. (D) Summary of M2R inhibition in the absence of PTX, pre-incubation of PTX and iPTX and PTX by no receptor is illustrated.

Figure 4. PTX effects on M1R mediated inhibition of Ca$_V$2.2(β2a).

(A) Time course recording of current inhibition by M1R activation with Oxo-M (10 μM) in cells expressing Ca$_V$(β2a) and pre-incubated in PTX. (B) Time course recording of current inhibition in the cells transfected with Ca$_V$(β2a) pre-incubated in denatured PTX (iPTX). (C) Current recording in control cells

following pre-incubation of PTX transfected with $Ca_V(\beta 2a)$ and absence of M1R. (D) Quantification of M1R inhibition (%) of $Ca_V(\beta 2a)$ with PTX, iPTX and no PTX.

5. FIGURES

Fig. 1. GPCR Modulation of Ca$_V$2.2(β2a) channels

Fig. 2. Regulation of Ca$_V$2.2 channels by PIP$_2$ depletion

Fig. 3. PTX effects on M2R mediated inhibition of Ca$_V$2.2(β2a)

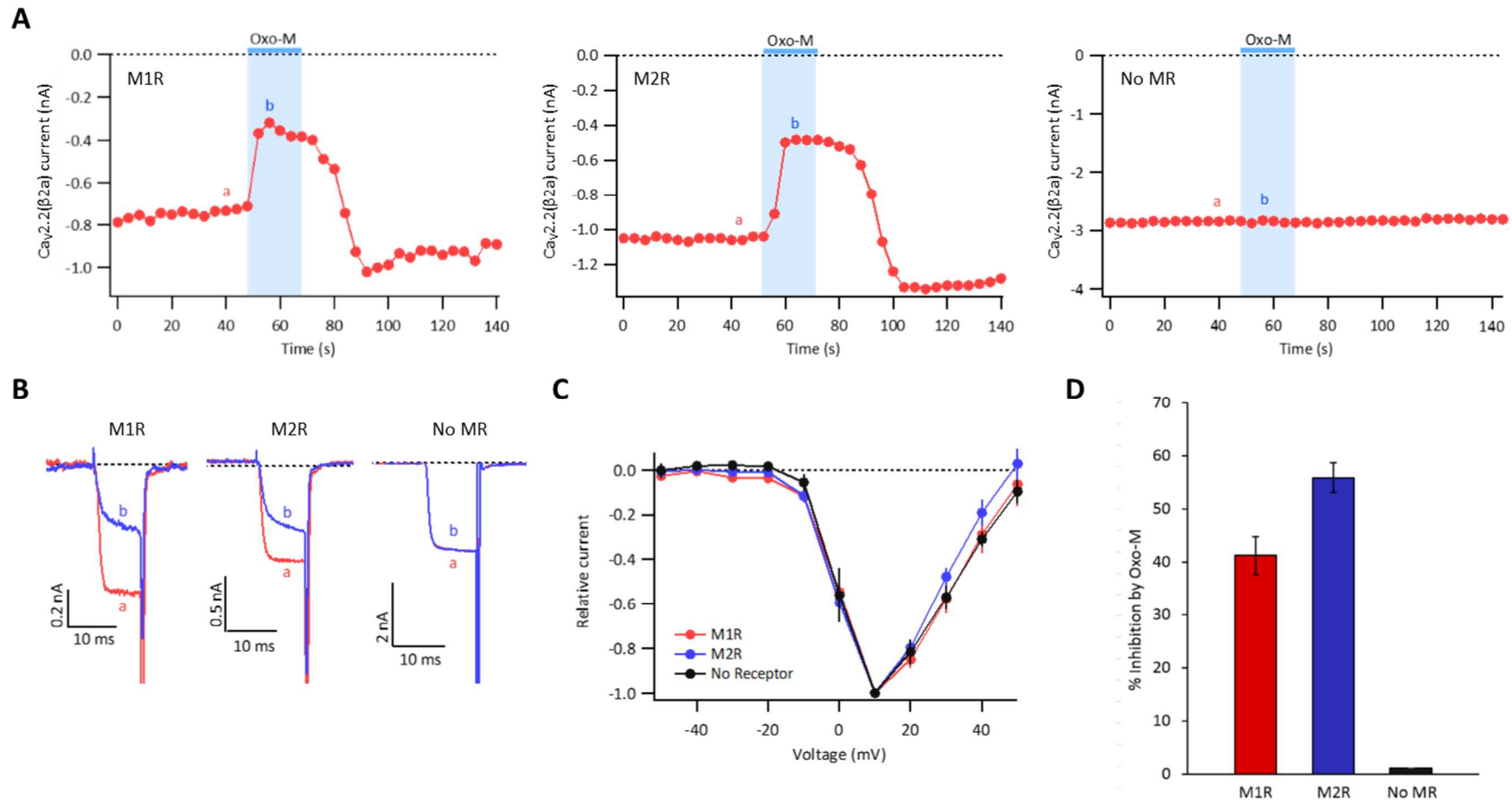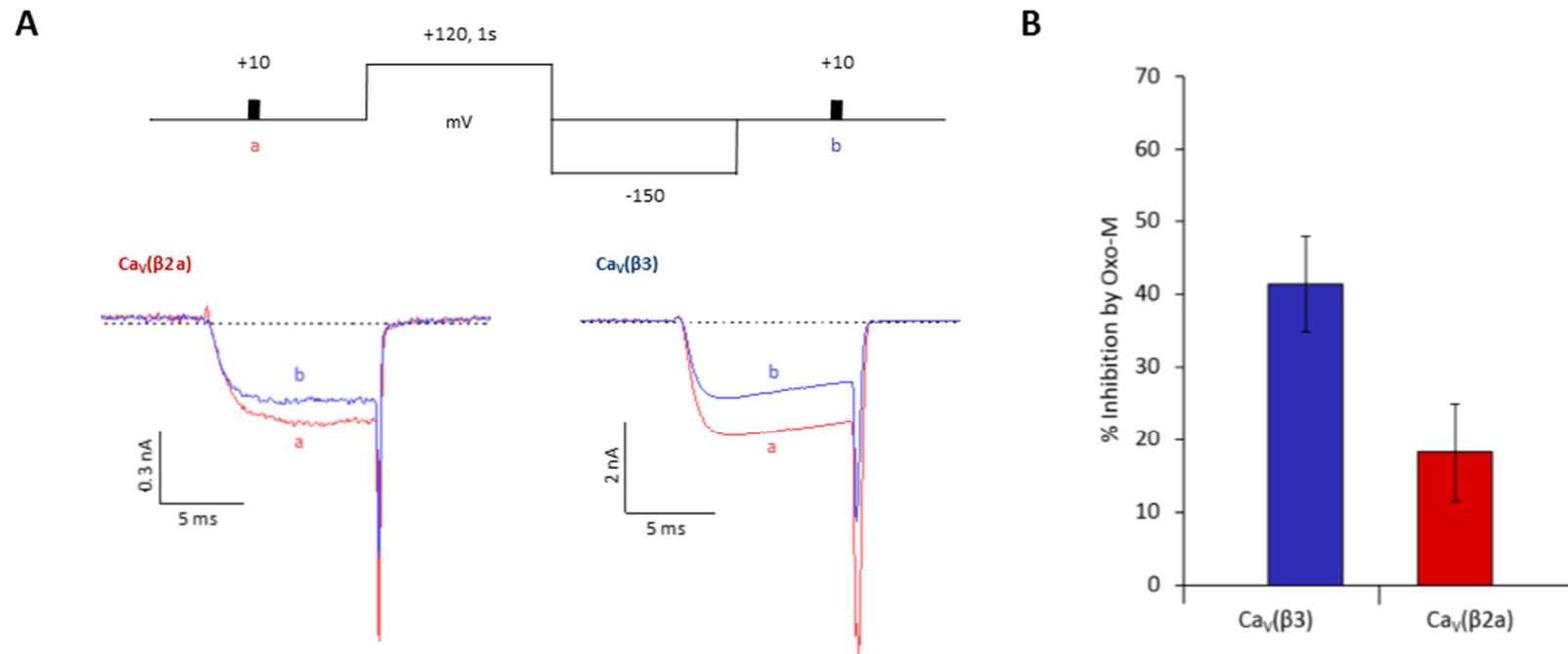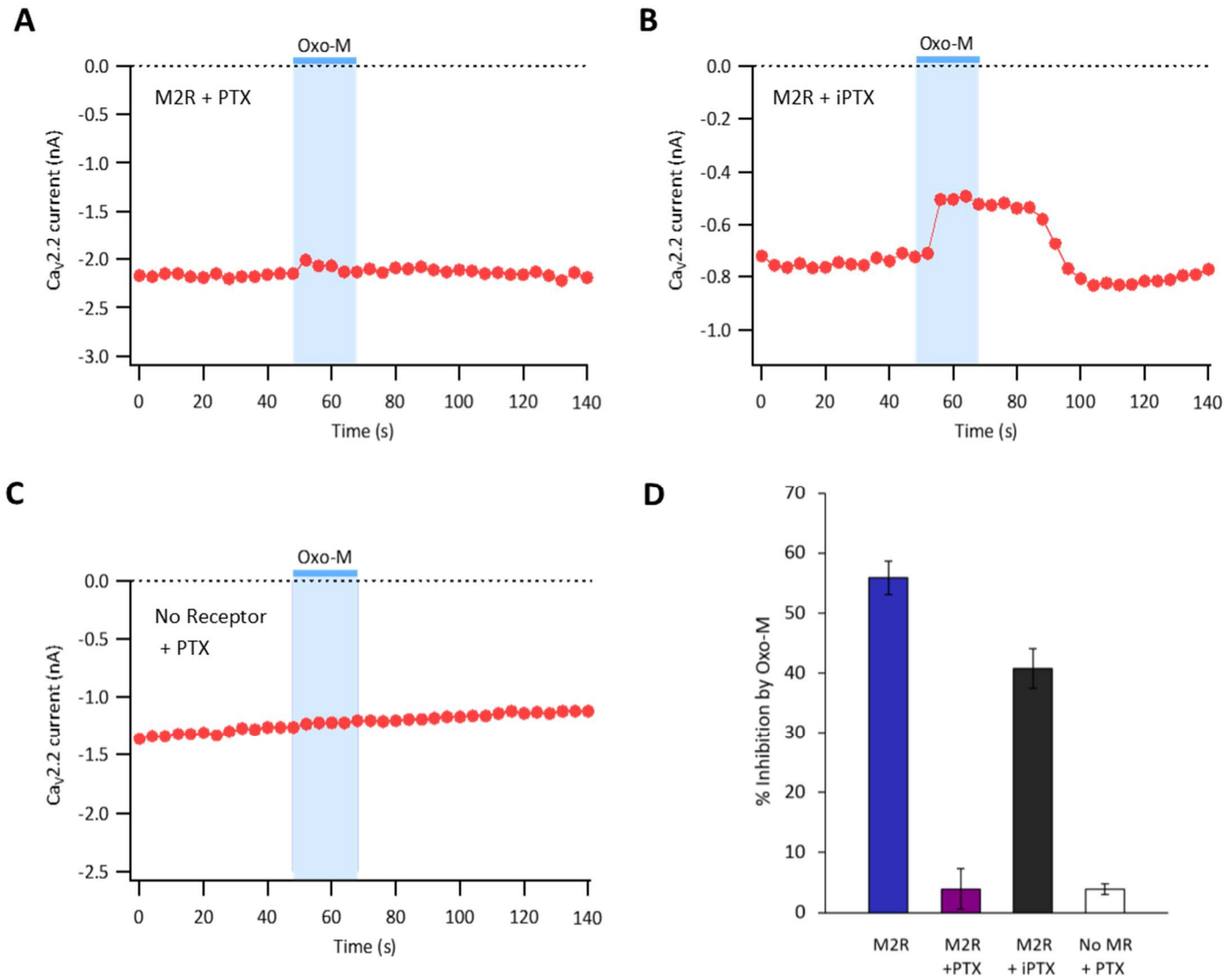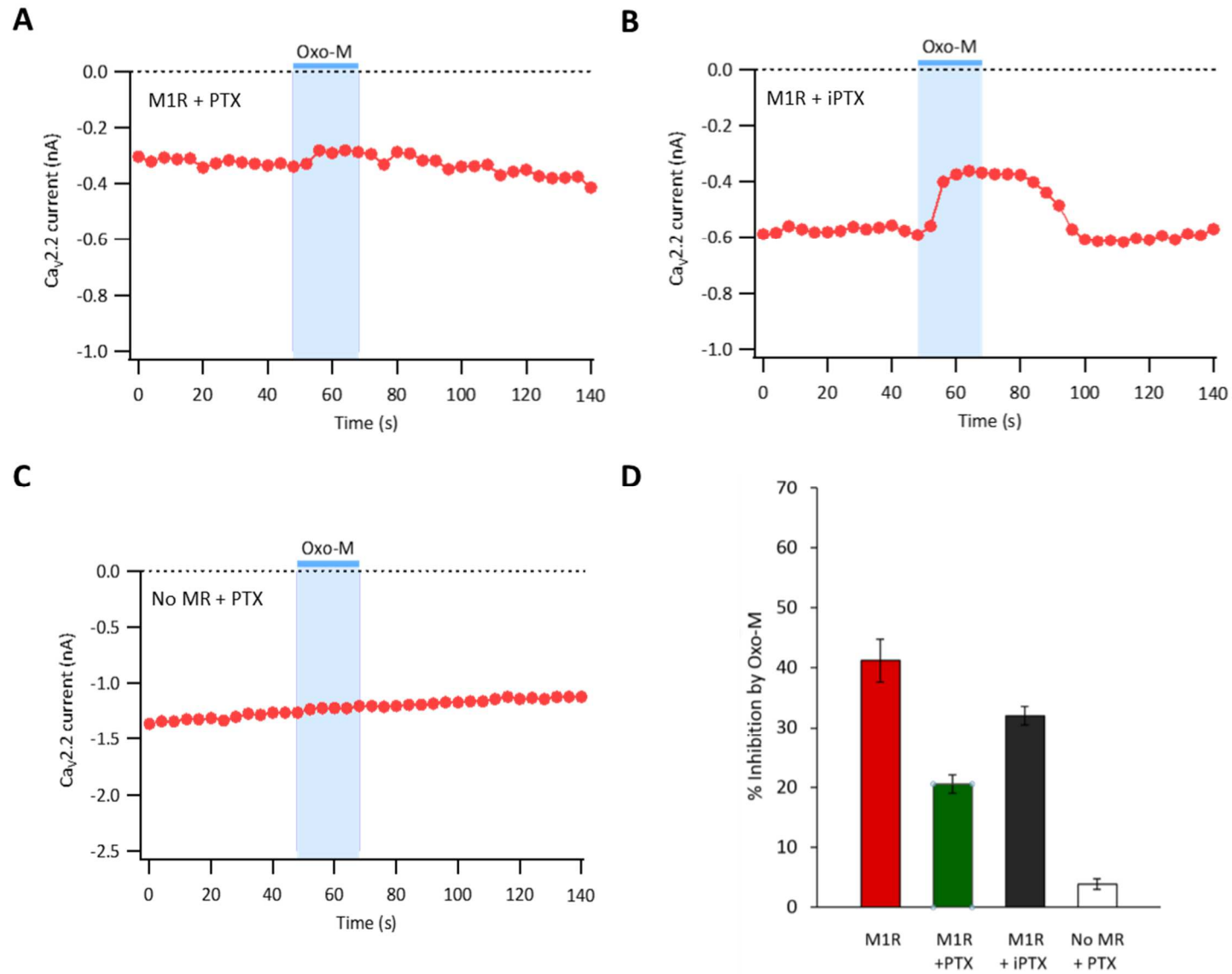**Fig. 4.** PTX effects on M1R mediated inhibition of $Ca_V2.2(\beta 2a)$

Chapter 2: Electrostatic residues in the Gβγ-dependent inhibition of GIRK2A channels

1. INTRODUCTION

Inwardly rectifying potassium channels (GIRK) play a crucial role in many types of excitable cells by allowing the specific efflux of potassium ions respectively [5]. This subsequently results in the hyperpolarization following GIRK channel activation [8]. This has several physiological implications. Studies with animal models suggest that GIRK has a critical role in pain perception and memory modulation. It has been implicated in altering the neuronal excitability and cell death, which is also related to epilepsy, Down's syndrome, Parkinson's disease and drug addiction [32] [33].

GIRK channels are also regulated by the GPCRs described in chapter 1. These channels are activated by the direct binding of Gβγ results in the activation of this channel and thus increase in the efflux of potassium ions [34].

GIRK channels are part of the G protein-coupled inwardly rectifying K^+ group of channels, also known as Kir3 [35]. GIRK channels are expressed as homo- or heteromeric combinations of different α subunits, GIRK 1 – 4, where GIRK1 does not function alone as a homomer [36]. In the mammalian neuron, GIRK

exists as a hetertetramer GIRK1/2 in the brain [37]. These channels exist on dendritic branches, spines and shafts in the postsynaptic densities of excitatory synapses in many central neurons [38]. Each subunit consists of only two transmembrane domains and a pore-forming loop [39]. The GIRK channels studied in this paper is the GIRK2A channels. The question of this study was developed following a paper published in Nature in 2013 where the crystal structure of the GIRK2 and Gβγ subunit was elucidated to a resolution of 3 Å using x-ray crystallography [40].

From this paper, the sequence alignment of amino acids at the binding interface of GIRK2A and Gβγ was revealed. Within the family of GIRK channels, the amino acids were highly conserved between the GIRK1-4 subunits, as well as other potassium channels of the larger family. This was interesting to note, as of the large family of potassium ion channels, only GIRK channels have been established to be directly activated by the binding of the Gβγ protein. However, of these highly conserved amino acid sequences between the GIRK1-4 subunits, few distinct differences were observed in the GIRK1 and GIRK2 subunits. GIRK1 lacked the conserved electrostatic residues found in the rest of the GIRK subunits. Thus, the question formulated from this study was how these specific amino acids affect the binding of Gβγ and thus the characteristics of GIRK channel activation [40]. It was hypothesized that the electrostatic residues present in GIRK 2-4 but not GIRK1 may have a role in the activation extent and kinetics of GIRK channels upon $G_{i/o}$PCR activation.

This investigation is relevant for the formation of GIRK channels. The GIRK2 subunit is known to form and function as homotetramers, however GIRK1 is not able to do so, rather it requires other GIRK subtypes to be present to form heterotetramers. This is also the conformation which is found more in the human body, GIRK1/2 in the brain and GIRK1/4 in the heart [41], and thus, much more physiologically relevant [42].

To study this, molecular biological techniques were implemented to perform specific site-directed mutagenesis to substitute the charged or polar amino acids in GIRK2 to resemble the amino acids in

GIRK1, which were uncharged or nonpolar. Electrophysiological recordings were used to study the total GIRK current activation and differences in activation kinetics of these wild type and mutant channels. These experiments were performed with co-transfected M_2 muscarinic receptors, as this is a $G_{i/o}$PCR, which is known to release Gβγ upon activation for the direct voltage-dependent activation of the GIRK channels [43] [44] [45].

2. MATERIALS AND METHODS

2.1. Expression of calcium and GIRK channels in mammalian cell lines

To study the GIRK channel and chimeras, the relevant genes were transfected into mammalian cell lies for expression.

2.1.1. Mammalian Cell lines

For studying the GIRK channels, cDNA encoding for the channel subunits, GIRK2A (from Eitan Reuveny, Weizmann Institute, RH), produced mutants GIRK/E358A;E350K and GIRK/T339F were transfected into the same tsA201 cells described above. Human M2-muscarinic receptor and Dr-VSP described in chapter 1 (Chapter 1, Section 1.1.1, Page 4) were used simultaneously.

These experiments were also carried out in human embryonic kidney cell line derivative tsA201-cells (HEK tsA-201 cells) using heterologous expression by transfection (Chapter 1, Section 1.1.1, Page 4)

2.1.2. Passage of tsA201 Cell Line

Refer to section 2.1.2 in Chapter 1 (Page 5)

2.1.3. Lipofectamine transfection

Refer to section 2.1.3 in Chapter 1 (Page 5)

For GIRK channel expression, 0.6 µg of either the WT GIRK2A channel or mutant GIRK channels were transfected. For both types of channels, relevant receptors 0.8 µg of M1R or M2R, 0.8 µg Dr-VSP and 0.1 µg of dsRed a fluorescent marker were also transfected as required.

2.1.4. Transfer of transfected tsA201 cells to Poly-L-Lysine coated chips

Refer to section 2.1.4 in Chapter 1 (Page 5)

2.2. Electrophysiological Recordings

Electrophysiological method recordings, using the whole cell patch clamping mode was conducted to study the activity of ion channels in cell membranes.

2.2.1. Solutions and Materials

To measure GIRK channel current, external low K^+ solution containing, 140 mM NaCl, 5.6 mM KCl, 1.2 mM $MgCl_2$, 2.6 mM $CaCl_2$, 10 mM HEPES, 2.6 mM Glucose and pH adjusted to 7.4 using NaOH. The high K+ external solution contained 140 mM KCl, 1.2 mM $MgCl_2$, 2 mM $CaCl_2$, 10 mM HEPES, 0.33 mM NaH_2PO_4, 10 mM Glucose adjusted to 7.4 using KOH. The pipette solution contained 107 mM KCl, 1.2 mM $MgCl_2$, 5 mM HEPES, 30 mM Sucrose, 2 mM Mg_2ATP, 0.3 mM Na_3GTP, adjusted to pH 7.2 with KOH, final K+ concentration 140 mM.

2.2.2. Whole cell recording

Refer to section 2.2.2 in Chapter 1 (Page 6)

Cells successfully transfected with GIRK channels were identified by red fluorescence, emitted by RFP due to the transfected dsRed gene.

To study the activity of GIRK channels, potassium currents were recorded by holding the cell at -80 mV and applying 10-ms test pulses at a frequency of 20Hz. In all experiments where potassium currents were

measured with a 10-ms test pulse, the full protocol induced p/5 subtraction of leak and capacitive currents.

2.2.3. Data analysis

Refer to section 2.2.3 in Chapter 1 (Page 8)

2.3. Site-directed mutagenesis on wild type GIRK2A channels

To study the GIRK2A mutants, wild type *GIRK2A* gene in pcDNA was used to perform site-directed mutagenesis at two specific sites using RF-PCR, short for Restriction-free PCR. This method provides a simple method to specifically insert a fragment of DNA into any location of a circular plasmid, independent of restriction sites or ligation. Different to other methods of site-directed mutagenesis, this technique introduces single mutations or small insertion/deletions to a plasmid in the absence of additional irrelevant residues. Diagram 1 illustrates this method [46]. A template DNA, in this case, pcDNA3.1 containing GIRK2 was used. The primer containing the specific substitutions were combined with the template DNA and RF-PCR performed. The first PCR product produces a megaprimer which is used in the second round of PCR to produce the mutations on the template DNA [47].
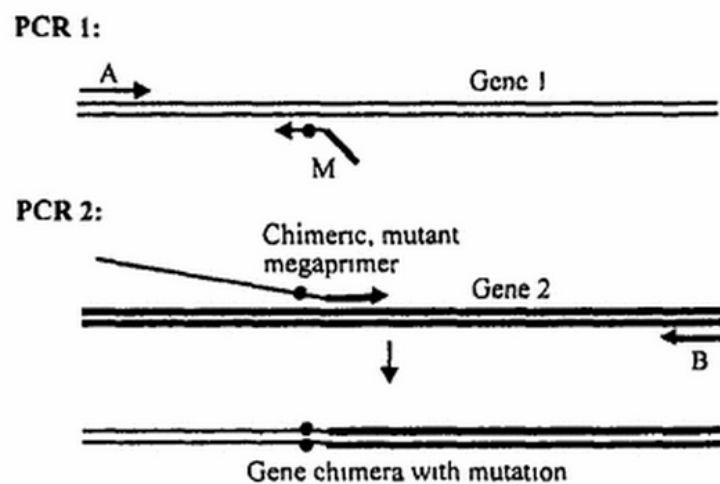

Diagram 1. The megaprimer method of site-directed mutagenesis

2.3.1. All-around Polymerase Chain Reaction to make Megaprimers

PCR (Polymerase Chain Reaction) was conducted to amplify DNA sequences for cloning and to perform site-directed mutagenesis experiments. All primers were ordered from Sigma-Aldrich and dissolved in deoxygenized water as a 10 µL working stock solution. Megaprimers were designed to allow the T338F or E359K;E358A mutations on each primer.

The primer sets used were, for the GIRK2A/E350K;E358A mutant,

TTCTACAAAGTTGACTACAACAGCTTCCATGCGACATATGAG (Forward) and

CTCATATGTCGCATGGAAGCTGTTGTAGTCAACTTTGTAGAA (Reverse).

To firstly produce the megaprimers the sense primer with mutation was added with an antisense primer of GIRK2A. PCR was run in normal conditions using a Thermal Cycler Model 7300 (Applied Biosystems). DNA was first denatured at 94°C for 2 min, then again for 30s, then annealed at 60°C for 30 s, and elongated at 72°C for 1 min, repeated for 25-40 cycles. A final DNA elongation step for 10 min at 72°C finished the cycle. PCR reagents such as Taq Polymerase were purchased from Applied Biosystems.

2.3.2. Quantification of Nucleic Acids, Agarose Gel Electrophoresis, DNA Digestion, DNA Purification

The megaprimers made were quantified using Thermo Scientific NanoDrop TM 1000 Spectrophotometer, which analyzes with a 2 µL sample. Agarose gel electrophoresis for DNA was carried out on 2% agarose gel concentration in TAE buffer. After checking for the relevant sizes of DNA, 1:10 of DPN:PCR product was added to digest the template DNA for 1 hour in 37°C. Agarose gel electrophoresis was performed again to check the size the vector containing the megaprimer of interest and used for another round of PCR. PCR containing samples with only the megaprimers were used. The same PCR protocol was used except for the elongation time being reduced to 15 s. 0.7% agarose gel was prepared for the gel electrophoresis and DPN digestion carried out accordingly. DNA purification was done by a DNA purification kit from QIAGEN and finally quantified.

For the PCR reactions, gradient PCR was used to analyze the PCR produces at a range of temperatures. DNA ranges from 50°C to 65°C was used.

2.3.3. Heatshock transformation, inoculation and extraction of DNA

To introduce the plasmid DNA with mutations into bacterial, chemical competent DH5a cells, 10 μL of PCR product was added to 100 μL of competent bacteria and left in ice for 5 mins. Heat shock was performed for 1 min at 42°C followed by ice for 5 min. 1 mL of LB without antibiotics was added and placed in the 37°C shaker incubator for 45 mins. After removing the supernatant from forming a palette, the suspended mixture was plated on Amplicillin agar plates and incubated overnight at 37°C.

Innoculation of colonies were left overnight and DNA extracted using a Mini-prep kit by Invitrogen. This Innoculation was performed in 4mL of LB media and 1% antibiotics with a swab of a single colony. The miniprep process was followed using the protocol provided by Invitrogen. This consisted of preparing the cell lysate using lysis buffer and precipitation buffer, then binding and washing the DNA using the wash buffers and eluting and precipitating DNA to finally derived DNA from the mixture.

3. RESULTS AND DISCUSSION

3.1. GIRK2A channel activation following M_2R activation

The extent and kinetics of GIRK2A channel activation following M2R, a $G_{i/o}$PCR was investigated using co-transfected tsA201 cells with GIRK2A subunits and M2R. A low 5.6 M potassium external solution was first used to maintain the cells in a physiologically similar concentration while the whole-cell was made. However following perfusion of a higher 140 mM potassium external solution, the basal current activation of GIRK2A channel was observed (Figure 1 *A*). This was as expected as the higher concentration of potassium outside the cell causes an electrochemical gradient which results in the inflow of potassium ions to the inside of the cell. Following activation of the M2R by perfusion of Oxo-M, an induced current could be observed which is indicative of fully opened GIRK2A channels. A relatively fast activation and slow deactivation can be observed (Figure 1 *A*).

The percentage of current contributed by the basal and induced component was calculated for these experiments (Figure 1 *C*). This clearly suggested the induced current made up for 92 ± 4 % of the total GIRK current activation where as the basal current showed to be 8.13 ± 4 % of the total GIRK current. The activation kinetics between the basal and the induced current measured by the τ value, measuring the time to reach the half maximal value of 100% current activation, did not have a significant difference. The τ value was calculated to be 22 ± 7 s and 16 ± 4 s for the basal and induced current respectively (Figure 1 *D*).

The extent of current inhibition following M2R activation, and was also calculated using the current density (Figure 1 *E*). The basal current showed very little current density at 5 ± 2 pA/pF, however, the induced current measured to be a much larger value, at 117 ± 6 pA/pF. The total GIRK2A current density following M_2R activation was calculated to be 122 ± 6 pA/pF. The data suggests that the size of the induced activation of GIRK2A is much larger compared to the basal current, both in terms of the current density and the portion making up the percentage of total measured current.

In addition, a comparative experiment was performed to measure GIRK2A channels in the absence of

M2R. Here, both the basal and induced current showed minimal levels of current activation (Figure 1 *B*).

The current density was measured to be 0.53 ± 0.37 pA/pF and 2.6 ± 1.5 pA/pF for the basal and induced

current respectively. The total current following Oxo-M perfusion was calculated to be 5.9 ± 1.2 pA/pF.

Thus it can be gathered that there was no major difference in the basal current, understandably due to

the irrelevance of the activity of receptors in the recording of basal currents. More importantly, a major

decrease in induced current activation was observed, which strongly supports the necessity of M2R

activation for GIRK2A channel activation and opening to allow induced current to be recorded.

3.2. GIRK2A channels measured in the presence of PTX

To examine the function of the Gβγ subunit during the activation of GIRK2A channels following M2R

activation, cells expressing GIRK2A and M_2R were pre-incubated in PTX for 12-16 hours before their

currents were measured. The results visibly showed a significant reduction in the induced current

following activation of M2R (Figure 2 *A*). The percentage of total current made up by the induced current

portion considerably reduced to 37 ± 7 % and basal accounted to be the remaining 63 ± 7 % (Figure 2 *D*).

Furthermore, the activation kinetics of induced current measured by the τ value, increased by two-fold to

48 ± 10 s and basal remained to be at 26 ± 6 s, which was similar to that in control conditions (Figure 2 *B*).

The slower opening of GIRK2A channels during the activation of induced current in the presence of PTX

corresponds to the importance of Gβγ during the fast opening of GIRK2A channels following activation of

M2R in control conditions.

A more drastic difference in current density was observed for the activated GIRK2A channel in the

presence of PTX. The current density values for the control condition (in the absence of PTX) and in the

presence of PTX is compared in Figure 2 *C* The current density for the basal current remained similar to

that in control conditions, measuring to be 3.3 ± 0.9 pA/pF. This is comprehendible as the basal current is

only a change in extracellular concentration of potassium and not dependent on the activation of the M2R.

On the other hand, the current density of the induced current dramatically decreased to 3.0 ± 1.5 pA/pF

compared to that of the control condition. The presence of PTX, which inhibits the Gβγ dissociation from

the activated G protein coupled to the M2R had a crippling effect on both the size and activation kinetics of the induced GIRK2A current but not the basal current. The current was size was diminished and the activation kinetics slowed down. These findings suggest that the mechanism by which GIRK2A channel activation occurs following M2R, a $G_{i/o}$PCR is indeed, highly likely due to the operation of Gβγ dissociated from the activated coupled G protein.

3.3. $G_{i/o}$PCR activation of GIRK2A mutants

To study the role of electrostatic amino acids at the site of the Gβγ-GIRK2A binding interface, site-directed mutagenesis was performed to GIRK2A to produce a mutant GIRK2 channel, E350K (negative to positive) and E358A (negative to hydrophobic). The original amino acids on GIRK2 were conserved in the Gβγ dependent GIRK2-4 subunits but not in the also Gβγ dependent GIRK1. The replaced amino acids resembled the amino acids present in GIRK1 to explore the differences which may be present in Gβγ dependent activation of GIRK channels. The GIRK2A/E350K;E358A mutant was co-transfected with M2R and current measured (Figure 3 *A*). The current density measured for these mutants illustrated a drastic decrease in current density for the induced current, 24 ± 6 pA/pF compared to the control conditions (Figure 3 *C*). However, the basal current remained to show a similar current density at 3.3 ± 1.7 pA/pF. This again suggests that only the induced current was affected by the manipulation of the electrostatic amino acids at the Gβγ-GIRK2 binding interface. The decrease in current density proposes the significant role of these electrostatic amino acids during the binding of the Gβγ for full activation of the GIRK2A channels.

However, it is interesting to note, both the tau value for the induced current did not change, 15 ± 3 s, whereas the time for the basal current decreased to 11 ± 1 s (Figure 3 *B*). Furthermore, the percentage of total current made up by the basal and induced current showed no major changes at 14 ± 3 % for the basal and 86 ± 3 % for the induced current. Figure 3 *D* illustrates the percentage of current made up by the basal and induced current during the perfusion of high K^+ and low K^+ solutions respectively.

The data presented strongly suggests that the extent of activation of GIRK2 channels are largely dependent on the presence of the electrostatic amino acids present within the binding interface of the channel and Gβγ. There was a significant decrease in the activation of the GIRK2A/E350K;E358A mutants following M2R activation which suggests that the binding of the Gβγ and GIRK2 channel was interfered with. It can be deduced that the binding affinity of Gβγ to the channel was impeded which lead to the disruption of potassium ion flux. However, the questions as to if the channel's pore opening was restricted in terms of number of channels open or the open probability of one channel is unknown. From the data presented, as there was no change in the activation kinetics of GIRK2A mutant channels, it can be suggested that the open probability is more likely to have changed. However many more studies need to be performed to validate this deduction. Thus, his study provides new avenues for which these concepts can be explored.

4. Figure Legends

Figure 1. Activation of GIRK2A channels with M2R

(A) GIRK2A channel currents induced by the activation of M2R rapidly activate following addition of 10 uM (Oxo-M). (B) Current in control cells expressing GIRK2A but no receptor is recorded. (C) A bar graph summarizing the current inhibition of total current (%) is presented. The basal current in the presence of high K^+ and induced current following M2R activation is presented. (D) Measurements of activation kinetics (τ, s) compared between the basal and induced current following M2R activation. (E) Summary of basal and induced current density (pA/pF) in the presence and absence of M2R is presented.

Figure 2. **Effect of PTX on modulation of GIRK2A channels**

(A) Time course current recording of cells expressing GIRK2A and M2R following pre-incubation in PTX. (B) Activation kinetics (τ, s) of the basal and induced GIRK2A current in the presence of PTX. (C) Summary of current density (pA/pF) of GIRK2A expressing cells in the presence and absence of PTX is presented. (D) Percentage of total current made up by the basal and induced current in the presence of PTX in cells expressing GIRK2A and M2R is summarized.

Figure 3. Modulation of GIRK2A/E350K;E358A by M2R

(A) GIRK2A/E350K;E358A current recordings show the basal current following high Potassium soluation of induced current following activation of M2R by 10 μM. (B) Activation kinetics (τ, s) of the basal and induced currents in cells expressing GIRK2A/E350K;E358A and M2R is presented in a bar plot. (C). Summary of the current density (pA/pF) of basal and induced current in cells expressing the mutant GIRK2A and M2R compared with that of wild type GIRK2A cells. (D) The basal and induced current proportions of the total current (%) is represented in the bar graphs.
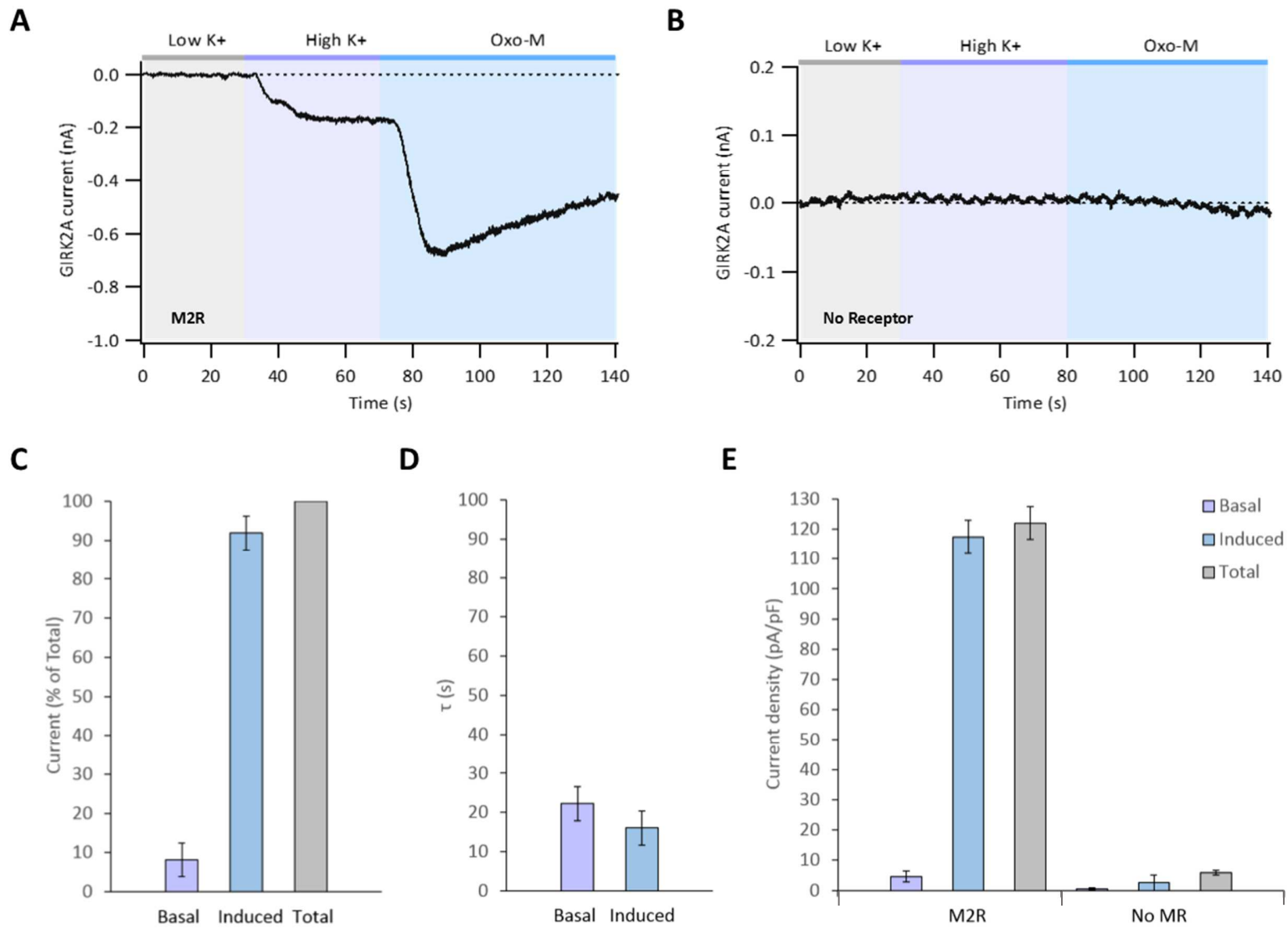
5. Figures

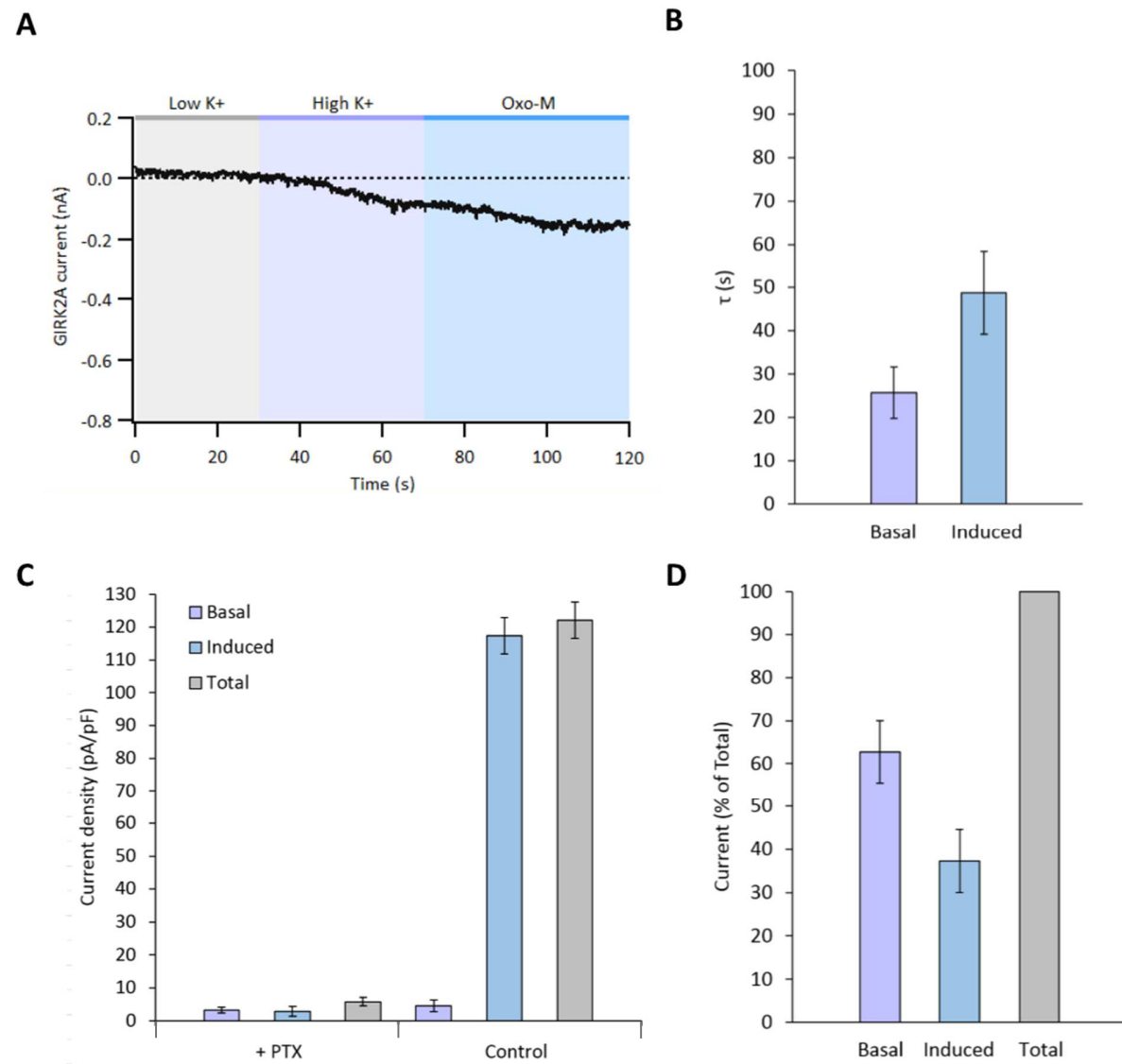**Fig. 1.** Activation of GIRK2A channels with M2R

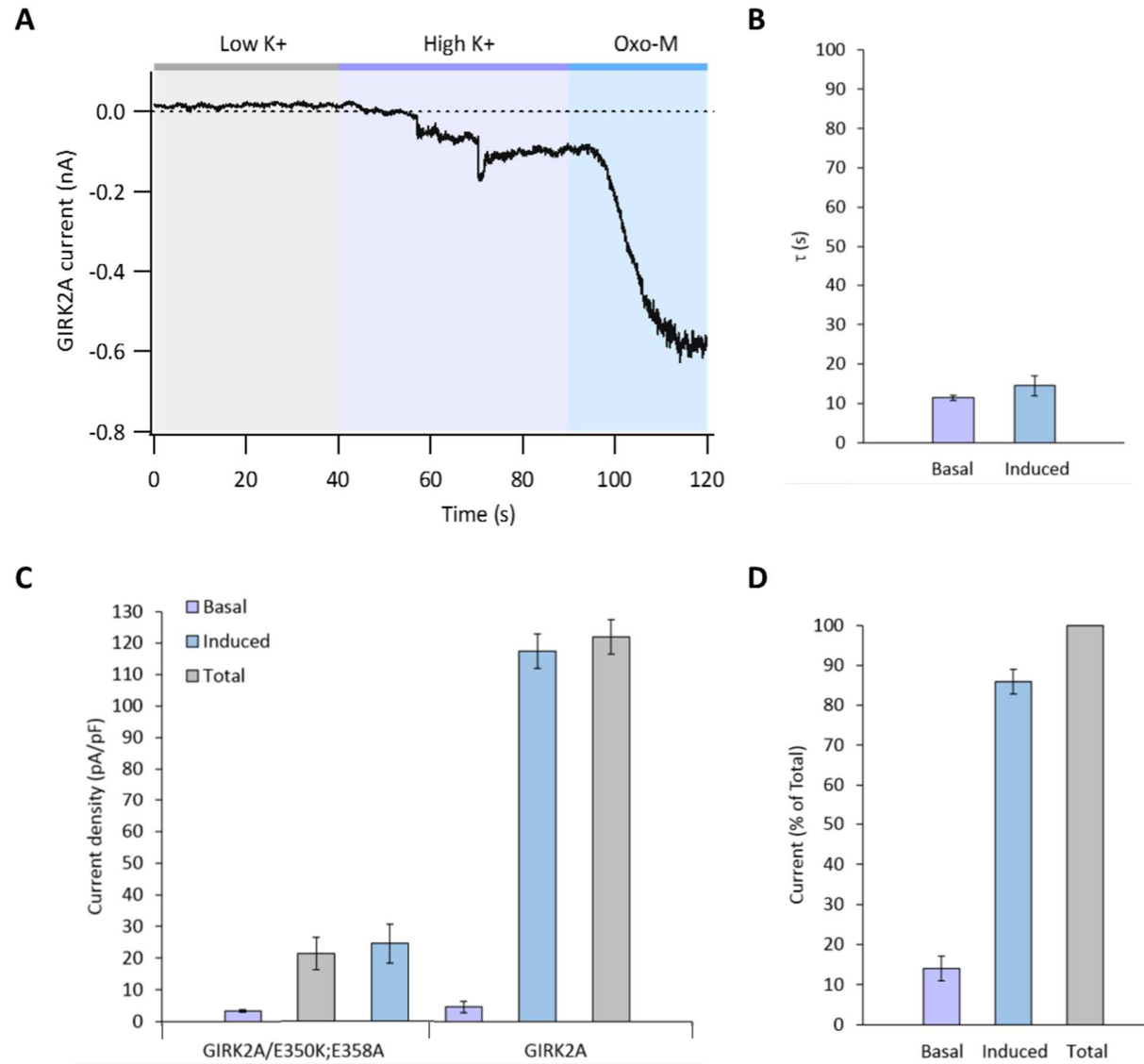**Fig. 2.** Effect of PTX on modulation of GIRK2A channels

Fig. 3. Modulation of GIRK2A/E350K;E358A by M2R

REFERENCES

1.   Catterall, W.A. and A.P. Few, *Calcium channel regulation and presynaptic plasticity.* Neuron, 2008. 59(6): p. 882-901.

2.   Zamponi, G.W. and T.P. Snutch, *Modulation of voltage-dependent calcium channels by G protein.* Current Opinion in Neurobiology, 1998. 8: p. 351-356.

3.   Roberts-Crowley, M.L., et al., *Regulation of voltage-gated Ca^{2+} channels by lipids.* Cell Calcium, 2009. 45(6): p. 589-601.

4.   Balla, T., *Phosphoinositides: Tiny lipids with giant impact on cell regulation.* Physiological Reviews, 2013. 93.

5.   Whorton, M.R. and R. MacKinnon, *Crystal structure of the mammalian GIRK2 K^+ channel and gating regulation by G proteins, PIP_2, and sodium.* Cell, 2011. 147(1): p. 199-208.

6.   Thiele, A., *Muscarinic signaling in the brain.* Annu Rev Neurosci, 2013. 36: p. 271-94.

7.   Sheng, J., et al., *Calcium-channel number critically influences synaptic strength and plasticity at the active zone.* Nat Neurosci, 2012. 15(7): p. 998-1006.

8.   Torres, G., R. Gainetdinov, and M. Caron, *Plasma membrane monoamine transporters: structure, regulation and function.* Nature Reviews Neuroscience, 2003. 4: p. 13-25.

9.   Lipscombe, D., S. Kongsamut, and R. Tsien, *Alpha-adrenergic inhibition of sympathetic neurotransmitter release mediated by modulation of N-type calcium-channel gating.* Nature, 1989. 340: p. 639-642.

10.   Khanna, R., et al., *The presynaptic $Ca_V2.2$ channel-transmitter release site core complex.* Eur J Neurosci, 2007. 26(3): p. 547-59.

11.   Catterall, W.A., *Structure and regulation of voltage-gated Ca^{2+} channels.* Annual Review of Cell and Developmental Biology, 2000. 16: p. 521-55.

12.   Lipscombe, D., S.E. Allen, and C.P. Toro, *Control of neuronal voltage-gated calcium ion channels from RNA to protein.* Trends Neurosci, 2013. 36(10): p. 598-609.

13.   Zamponi, G.W. and K.P. Currie, *Regulation of Ca$_V$2 calcium channels by G protein coupled receptors.* Biochim Biophys Acta, 2013. 1828(7): p. 1629-43.

14.   Chini, B., et al., *G-protein-coupled receptors - from structural insights to functional mechanisms.* 2013. 41: p. 135-136.

15.   Hulme, E.C., *GPCR activation: a mutagenic spotlight on crystal structures.* Trends Pharmacol Sci, 2013. 34(1): p. 67-84.

16.   Bjarnadottir, T.K., et al., *Comprehensive repertoire and phylogenetic analysis of the G protein-coupled receptors in human and mouse.* Genomics, 2006. 88(3): p. 263-73.

17.   Betke, K., C. Wells, and H. Hamm, *GPCR mediated regulation of synaptic transmission.* Progress in Neurobiology, 2012. 96(3): p. 304-321.

18.   Nobles, M., A. Benians, and A. Tinker, *Heterotrimeric G proteins precouple with G protein-coupled receptors in living cells.* Proc Natl Acad Sci U S A, 2005. 102(51): p. 18706-11.

19.   Herlitze, S., et al., *Modulation of voltage-dependent calcium channels by G protein.* Nature, 1996. 380: p. 258-262.

20.   Ikeda, S.R., *Voltage-dependent modulation of N-type calcium channels by G-protein β γsubunits.* Nature, 1996. 380: p. 255-258.

21.   Hille, B., *Modulation of ion-channel function by G-protein-coupled receptors.* Trends in Neuroscience, 1994. 17(12): p. 531-536.

22.   Gohar, O., *Ion Channel Modulation by G-Protein Coupled Receptors.* Modulator, 2006. 21: p. 2-8.

23.   Bernheim, L., D. Beech, and B. Hille, *A Diffusible Second Messenger Mediates One of the Pathways Coupling Receptors to Calcium Channels in Rat Sympathetic Neurons.* Neuron, 1991. 6: p. 859-867.

24.   Delmas, P., et al., *Phosphoinositide lipid second messengers: new paradigms for calcium channel modulation.* Neuron, 2005. 47(2): p. 179-82.

25.   Suh, B.C., K. Leal, and B. Hille, *Modulation of high-voltage activated Ca^{2+} channels by membrane phosphatidylinositol 4,5-bisphosphate.* Neuron, 2010. 67(2): p. 224-38.

26.   Suh, B.C., et al., *Membrane-localized beta-subunits alter the PIP2 regulation of high-voltage activated Ca2+ channels.* Proc Natl Acad Sci U S A, 2012. 109(8): p. 3161-6.

27. Raingo, J., A. Castiglioni, and D. Lipscombe, *Alternative splicing controls G protein–dependent inhibition of N-type calcium channels in nociceptors.* Nature Neuroscience, 2007. 10: p. 285-292.

28. Neher, E., *Ion Channels for Communication Between and Within Cells* Bioscience Reports, 1991. 12(1).

29. Molleman, A., *Patch Clamping: An Introductory Guide to Patch Clamp Electrophysiology*. 2003: John Wiley & Sons, Ltd.

30. Martin, R., *Neuroscience Methods: A Guid for Advanced Students*. 1997, The Netherlands: Harwood Academic Publishers.

31. Clancy, S.M., et al., *Pertussis-toxin-sensitive Galpha subunits selectively bind to C-terminal domain of neuronal GIRK channels: evidence for a heterotrimeric G-protein-channel complex.* Mol Cell Neurosci, 2005. 28(2): p. 375-89.

32. Lujan, R., et al., *New insights into the therapeutic potential of Girk channels.* Trends Neurosci, 2013.

33. Luscher, C. and P.A. Slesinger, *Emerging roles for G protein-gated inwardly rectifying potassium (GIRK) channels in health and disease.* Nat Rev Neurosci, 2010. 11(5): p. 301-15.

34. Riven, I., S. Iwanir, and E. Reuveny, *GIRK channel activation involves a local rearrangement of a preformed G protein channel complex.* Neuron, 2006. 51(5): p. 561-73.

35. Kubo, Y., et al., *International Union of Pharmacology. LIV. Nomenclature and molecular relationships of inwardly rectifying potassium channels.* Pharmacol Rev, 2005. 57(4): p. 509-26.

36. Mase, Y., et al., *Structural basis for modulation of gating property of G protein-gated inwardly rectifying potassium ion channel (GIRK) by i/o-family G protein alpha subunit ($G\alpha_{i/o}$).* J Biol Chem, 2012. 287(23): p. 19537-49.

37. Guillemare, E., *Molecular Properties of Neuronal G-protein-activated Inwardly Rectifying K^+ Channels.* Journal of Biological Chemistry, 1995. 270(48): p. 28660-28667.

38. Lujan, R., J. Maylie, and J.P. Adelman, *New sites of action for GIRK and SK channels.* Nat Rev Neurosci, 2009. 10(7): p. 475-80.

39. Doyle, D., et al., *The Structure of the Potassium Channel: Molecular Basis of K^+ Conduction and Selectivity.* Science, 1998. 280: p. 69-77.

40.   Whorton, M.R. and R. MacKinnon, *X-ray structure of the mammalian GIRK2-βγ G-protein complex.* Nature, 2013. 498(7453): p. 190-7.

41.   Krapivinsky, G., et al., *The G-protein-gated atrial K⁺ channel IKAch is a heteromultimer of two inwardly rectifying K⁺-channel proteins.* Nature, 1995. 374: p. 135-141.

42.   Reuveny, E., *Ion channel twists to open.* Nature, 2013. 498: p. 182-183.

43.   Raveh, A., et al., *Nonenzymatic rapid control of GIRK channel function by a G protein-coupled receptor kinase.* Cell, 2010. 143(5): p. 750-60.

44.   Nemec, J., K. Wickman, and D. Clapham, *Gβγ binding increases the open time of IKACh - kinetic evidence for multiple Gβγ binding sites.* Biophysical Journal, 1999. 76: p. 246-252.

45.   Zylbergold, P., N. Ramakrishnan, and T. Hebert, *The role of G proteins in assembly and function of Kir3 inwardly rectifying potassium channels.* Channels (Austin), 2010. 4(5): p. 411-21.

46.   Barik, S., *Methods in Molecular Biology - From Molecular Cloning to Genetic Engineering.* Methods in Molecular Biology, ed. B. White. 1997: Humana Press.

47.   Ent, V.L., J., *RF cloning: A restriction-free method for inserting target genes into plasmids.* Journal of biochemical and biophysical methods, 2006. 67: p. 67-774.

ABSTRACT IN KOREAN

요약문

이온채널은 세포의 안과 밖으로 이온의 선택적인 투과를 가능하게 하며 특정한 GPCR 에 의해 정교하고 민감하게 조절된다. 이것은 흥분성 세포에서 막 전위를 중요한 생물학적 기능들로 전환 하는데 있어서 조절자 역할을 한다. 특정한 전압개폐칼슘채널인 $Ca_V2.2$ (N-type) 채널과 G-protein-coupled potassium 2A 채널 (GIRK2A) 모두 $G_{i/o}$-protein-coupled receptors ($G_{i/o}$PCRs)로 부터 분리된 $G\beta\gamma$의 직접적인 결합에 의해 조절된다.

이번 연구는 빠르고, 전압 의존적이며 세포막에서만 일어나는 이온 채널 조절 메커니즘이다. 첫 번째 부분에서, 다른 타입의 GPCR 활성화에 따른 하위 경로의 존재 가능성을 연구하였다. 이전의 연구들은 분리된 $G\alpha_q$ 단백질이 $Ca_V2.2$ 채널을 억제하기 위해 세포막으로부터 PIP_2 를 고갈시키며, 이러한 느리고, 전압에 비의존적이며, 지질 의존적인 경로 때문에 대부분 발생하는 GqPCR 활성화에 따른 분명한 억제 경로를 입증하였다. 그러나 $G\beta\gamma$ 의존적 경로 또한 $Ca_V2.2$ 채널 억제를 도울 수 있는 가능성으로 인해 기존에 알려진 메커니즘에 대해 다시 한번 생각해보아야 한다. 결과는 분명히 이 가설을 옹호한다. $Ca_V\beta2a$ current inhibition 에서 중요한 감소는 PTX 가 미리 처리된 cell 에서 측정되었다. PTX 는 $G_{i/o}$PCR 이며 또한 $G\beta\gamma$에 의한 G_qPCR 매개 $Ca_V2.2$ 채널 inhibition 에 역할을 하는 $G\beta\gamma$ blocker 이다.

두 번째 부분에서는, electrostatic residues 의 중요성이 GIRK1 소단위체가 아닌, GIRK2A 소단위체들과 $G\beta\gamma$의 결합 접점에 존재하는 것으로 최근에 발견되었다. 분자 생물학적 기술인 site-directed mutagenesis 를 이용하여 GIRK2A 채널의 세가지 돌연변이인, T338F(극성에서 소수성으로), E350K(음전하에서 양전하로), 그리고 E358A(음전하에서 소수성으로)를 만들었다. 모든 돌연변이들은 GIRK 와 $G\beta\gamma$의 결합 접점에 기여하는 것으로 보이는 GIRK1 의 아미노산과 비슷하다. GIRK 채널에서의 가장 흥미로운 점은 수많은 칼륨 채널들 중에서 $G\beta\gamma$와 결합하여서 활성화 되어진다고 알려진 유일한 칼륨 채널이다. 이런 차이점이 나타나는 이유는 아직까지 밝혀지지 않았다. 실험 결과, 보존된 아미노산의 중요성을 보여준 GIRK2A 돌연변이에서 상당한 current activation 의 감소를 실제로 보여준다. 게다가, GIRK 채널에서 GIRK1 은 생리학적으로 중요한 소단위체이다. 뇌에서는 GIRK1/2 heterotetramer 형태가 더 많이 존재하며, 심장에서는 GIRK1/4 heterotetramer 형태가 더 많이 존재한다. GIRK 채널에 $G\beta\gamma$가 결합함으로써 활성화되는 메커니즘을 자세히 알아보는 것은 흥미 있는 주제이다. 실험결과, wild-type 의 activation 정도와 비교하여 GIRK2 채널 mutants 의 activation 정도는 특징적 감소를 보여준다. 그러나 activation kinetics 에서의 변화는 관찰되지 않았다.

CURRIVULUM VITAE

Name   Christina (Dasom) Baek

Birth Date   6 July 1989

Education   M.S. Brain Science – Second year (2012 – Present)
Department of Brain Science
Daegu Gyeongbuk Institute of Science and Technology (DGIST)
Daegu, South Korea

B.S. Biomedical Science (2003 – 2007)
University of Auckland
New Zealand

Baradene College of the Sacred Heart (2003 – 2007)

Auckland, New Zealand

Research   A member of the Cellular and Molecular Neurobiology Lab,
Experience   Brain Science, DGIST under the Professor Byung-Chang Suh, Ph.D

Poster Presentations

2012 International Ion Channel Conference
"Negative modulation of voltage- gated Ca^{2+} channels is determined by their β subunits during M1 muscarinic receptor activation"
Daniel Keum*, Christina Baek*, Byung-Chang Suh
August 24 – 27, 2012
The Shilla Hotel, Jeju Island, Korea

Biophysical Society 57th Annual Meeting
"Negative modulation of voltage-gated Ca^{2+} channels is determined by their β subunits during M1 receptor activation"
Daniel Keum*, Christina Baek*, Byung-Chang Suh
February 2 – 6, 2013
Philadelpphia, Pennsylvania

Conference Attendance

2012 DGIF – DGIST Global Innovation Festival

Work Experience   TA in Methods in Neuroscience (2012)

Private Tutor for High School and College subjects. Biological Sciences, Chemistry, Physics, Mathematics in Calculus and in Statistics, English writing and reading (2006 – 2011)

Front Office Receptionist at the Quadrant Hotel
(2008 – 2011)

Voluntary Work at the Auckland Children's Hospital, Bernados Kindergarten, St Peter's Church for Autistic Children, Tutoring programs at public primary schools, Event managing administration and assistance for Red Carpet.
(2008 – 2011)

Awards   Scholarship Experience at the Weizmann Institute Summer Science School, Israel
DGIST President, Dr. Sung-Chul Shin's recommendation
Experience in Professor Eitan Reuveny's Laboratory of Biophysics and Ion Channel signaling

ABRSM Associated Board of the Royal Schools of Music – Grade 8 Pianoforte

College Awards:
Pender Cup – Senior Science award
Hawthorn Cup – Senior Mathematics award
Senior Chemistry Cup
Cor Unum Award – School spirit award
Distinction Awards in Chemistry and Calculus
Excellence Awards in Biology and Physics